



Reservoir quality evaluation of the Farewell sandstone by integrating sedimentological and well log analysis in the Kupe South Field, Taranaki Basin-New Zealand

S. M. Talha Qadri¹ · Md Aminul Islam² · Mohamed Ragab Shalaby^{2,3} · Ahmed K. Abd El-Aal⁴

Received: 7 September 2020 / Accepted: 23 October 2020 / Published online: 18 November 2020
© The Author(s) 2020

Abstract

The study used the sedimentological and well log-based petrophysical analysis to evaluate the Farewell sandstone, the reservoir formation within the Kupe South Field. The sedimentological analysis was based on the data sets from Kupe South-1 to 5 wells, comprising the grain size, permeability, porosity, the total cement concentrations, and imprints of diagenetic processes on the reservoir formation. Moreover, well log analysis was carried on the four wells namely Kupe South 1, 2, 5 and 7 wells for evaluating the parameters e.g., shale volume, total and effective porosity, water wetness and hydrocarbon saturation, which influence the reservoir quality. The results from the sedimentological analysis demonstrated that the Farewell sandstone is compositionally varying from feldspathic arenite to lithic arenite. The analysis also showed the presence of significant total porosity and permeability fluctuating between 10.2 and 26.2% and 0.43–1376 mD, respectively. The diagenetic processes revealed the presence of authigenic clay and carbonate obstructing the pore spaces along with the occurrence of well-connected secondary and hybrid pores which eventually improved the reservoir quality of the Farewell sandstone. The well log analysis showed the presence of low shale volume between 10.9 and 29%, very good total and effective porosity values ranging from 19 to 32.3% as well as from 17 to 27%, respectively. The water saturation ranged from 22.3 to 44.9% and a significant hydrocarbon saturation fluctuating from 55.1 to 77.7% was also observed. The well log analysis also indicated the existence of nine hydrocarbon-bearing zones. The integrated findings from sedimentological and well log analyses verified the Farewell sandstone as a good reservoir formation.

Keywords Farewell sandstone · Kupe South Field · Hydrocarbon saturation · Reservoir quality

Introduction

The hydrocarbon exploration and field development procedures are rapidly shifting toward the investigation of complex geological settings (Islam et al. 2020). This has resulted

in following the advanced procedures for enhancing production to meet the global energy requirements (Osinowo et al. 2018). Consequently, the integrated geological, geophysical and petrophysical schemes are used to establish the reservoir quality, thus estimating the important properties of the rock such as porosity, shale volume, net pay thickness and fluid saturation along with the impact of diagenetic phases on the reservoir formation (Adelua et al. 2019).

The Taranaki Basin is known for the hydrocarbon reserves discovered from numerous potential reservoir formations (Anthony et al. 2005). Kupe Gas Field (shown in Fig. 1) is among the 22 fields situated within the Taranaki Basin. The Farewell Formation is considered as a major hydrocarbon-bearing formation within the study area (Qadri et al. 2019a; Alotaby 2015). Various researchers have worked on the reservoir quality evaluation around the globe, by using multiple techniques i.e., structural, sedimentological, or petrophysical analyses. Some of the scientists have used one method (e.g.,

✉ S. M. Talha Qadri
talhaqadri_uos@hotmail.com

¹ Department of Earth Sciences, University of Toronto, Toronto, Canada

² Geoscience Program, Faculty of Science, Universiti Brunei Darussalam, Jalan Tungko Link, Gadong BE 1410, Negara Brunei Darussalam

³ Geology Department, Faculty of Science, Tanta University, Tanta 31527, Egypt

⁴ Faculty of Engineering, Najran University, P.O. Box 1988, Najran, Saudi Arabia

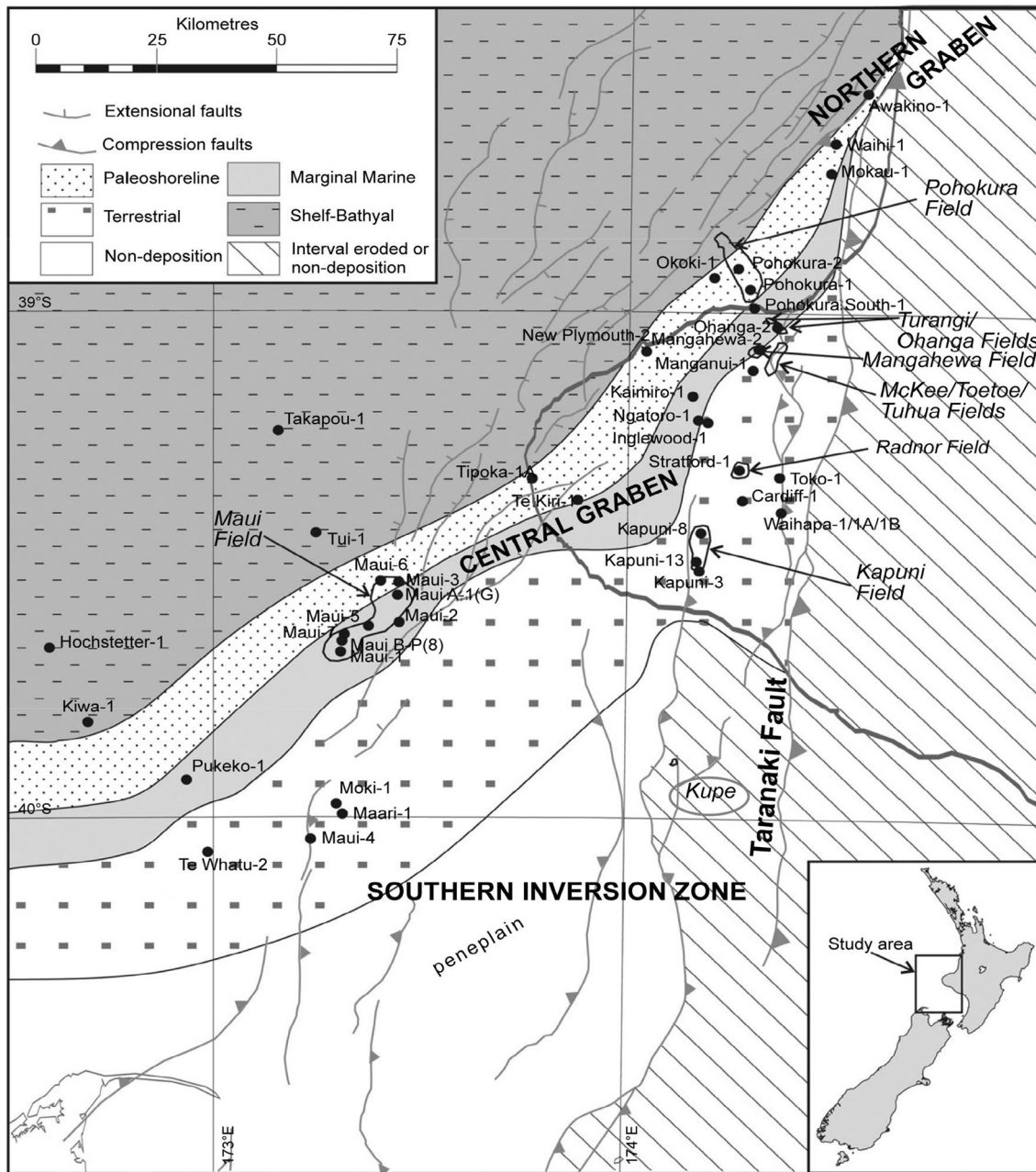


Fig. 1 Location map of the Eastern Mobile belt of the Taranaki Basin, indicating the structural features, different fields, specifying Kupe Field with a red ellipse in the Southern Inversion Zone (modified after Higgs et al. 2012)

Qadri et al. 2019b, 2017; Alotaby 2015, etc.), while others have integrated two or more methods (e.g., Al-Jawad et al. 2020; Islam et al. 2020; Nabawy et al. 2019; Soleimani et al. 2017; Islam 2009; Gier et al. 2008). A very limited number of scientists have focused on investigating the reservoir quality within New Zealand. The research by Martin et al. (1994), Griffin et al. (2015), Higgs et al. (2017) and Jumat et al. 2018 evaluated the reservoir quality on a basin scale, whereas very few studies (e.g., Dong et al. 2018; Shalaby et al. 2020) have utilized the integrated analysis to establish

the reservoir quality on a field scale within the Taranaki Basin, thus leaving behind an ample scope of conducting a detailed investigation using sedimentological and well log analyses to determine the reservoir quality of the Farewell Formation within the Kupe South Field. The sedimentological analysis highlights the texture, detrital mineralogy, diagenetic phases and their impact on the reservoir quality. The study also investigates the influential petrophysical parameters which control the reservoir quality. The findings and the knowledge obtained from this study will be implied

for reservoir characterization on the field and basin scale within the Taranaki Basin and other adjacent basins, using three-dimensional structural and petrophysical models, well log analysis and sedimentological analysis.

Geological settings

Taranaki Basin is one of the largest of a series of interconnected Cretaceous-Cenozoic sedimentary basins that extended along the western margin of New Zealand (King and Thrasher 1996). This is a subsurface basin lying offshore beneath the continental shelf (Strogen 2014). The Taranaki Basin comprises two major structural features i.e., the Western Stable Platform and the Eastern Mobile Belt (Knox 1982). The Eastern Mobile Belt has undergone a complex tectonic regime and contains up to 11 km of sedimentary strata (Alotaby 2015). The study area is in the south of the Eastern Mobile belt (Knox 1982). The Kupe Field shown in Fig. 1 is considered among the significant hydrocarbon reserves within the study area (King and Thrasher 1996). The Farewell sandstone belongs to the Pakawau Group deposited during the Paleocene epoch (Raine 1984). The Mangahewa Formation is a proven source rock, whereas the Otaraoa and NorthCape Formations act as the top and bottom seal, respectively, trapping the hydrocarbon accumulations (Qadri et al. 2016). Figure 2 illustrates the general stratigraphy of the study area. The wells encountering the Farewell Formation within the studied field display stacked thinning as well as fining upward deposition cycles, with a thickness of 150 to 200 m (Schmidt and Robinson 1990). Sandstones dominated the base of the depositional cycles while the mudstones deposited the top of the cycles (King and Thrasher 1996). The Farewell sandstones, in the study area, were deposited in a valley by a northward draining fluvial system, developed by the Manaia Fault system (Alotaby 2015).

Methodology

A generous contribution from the Ministry of Business, Innovation and Employment (MBIE), New Zealand, in the form of 66 core-based petrographical datasets, derived from the variable reservoir depths of the Kupe South-1 to 5 wells. Tables 1 and 2 show the data used to conduct the petrographical study and helped to understand the lithology, texture and detrital mineralogy of the reservoir formation. The reservoir quality was assessed by conducting statistical analysis and establishing the relationship among various parameters such as porosity, permeability, cement content, etc. Moreover, the influence of detrital mineralogy and cementation on the reservoir quality was

also assessed by using the photomicrograph from the Kupe Gas Field. The well log analysis was also performed over the four wells namely Kupe South 1, 2, 5 and 7 wells, to find the variation and dissemination of the key parameters which influence the reservoir quality. The shale-free zones where the pore spaces are filled with water or hydrocarbons, the neutron log estimates the fluid-filled porosity whereas the density log determines the overall density of rock including the solid matrix and the fluid within the pore spaces. The corrected porosity is then estimated by using a combination of density and neutron logs (Asquith and Krygowski 2004; Rider 1996) often termed as Neutron-Density Porosity Model within the Interactive Petrophysics 2013. To discriminate the zones of high porosity, a 10% cutoff was applied (Qadri et al. 2019b). The neutron tool response was used to estimate the neutron porosity, whereas the Wyllie equation (Wyllie 1963) was used to calculate the density porosity.

$$\phi_{\text{den}} = \frac{(\text{den}_{\text{ma}} - \text{den}_{\text{b}})}{(\text{den}_{\text{ma}} - \text{den}_{\text{f}})} \quad (1)$$

where ϕ_{den} is the porosity derived from the density log, den_{ma} is the matrix density, den_{b} is the bulk density while den_{f} is the mud filtrate density.

Wyllie's equation shown below was used to calculate the sonic porosity. The estimated sonic porosity was plotted against neutron-density log-derived porosity to find if the reservoir comprises intergranular, secondary or combination of both types of total porosity.

$$\phi_{\text{sonic}} = \frac{(\text{delT}_{\text{log}} - \text{delT}_{\text{ma}})}{(\text{delT}_{\text{fl}} - \text{delT}_{\text{log}})} \quad (2)$$

$$\phi_{\text{ND}} = \left[(\phi_{\text{D}}^2 + \phi_{\text{N}}^2)^{1/2} \right] \quad (3)$$

where ϕ_{sonic} indicates the sonic porosity, delT_{log} indicates the sonic log values, delT_{ma} shows the sonic travel time through the matrix material and delT_{fl} shows the sonic travel time through the fluids. In Eq. (3), ϕ_{ND} is neutron-density porosity, ϕ_{D} is the density porosity and ϕ_{N} is the neutron porosity estimated based on the response by neutron tool.

It is imperative to know the volume of shale while evaluating reservoir quality. The lower volume of shale inside the pore spaces indicates the possibility of good reservoir quality. In addition to shale concentration, it is essential to identify the kind of shale dissemination within the reservoir zones. This was established by plotting neutron-derived porosity against the density-derived porosity. The results indicated the presence of the dispersed shale, and therefore, dual water saturation scheme was applied to calculate the precise hydrocarbon saturation (S_{w}) within the studied wells. To discriminate the shale rich regions from the sand-rich sectors within the reservoir formation, a fifty per cent cutoff was used. This means that the interval contains 50% or above shale content will be considered as non-reservoir zone

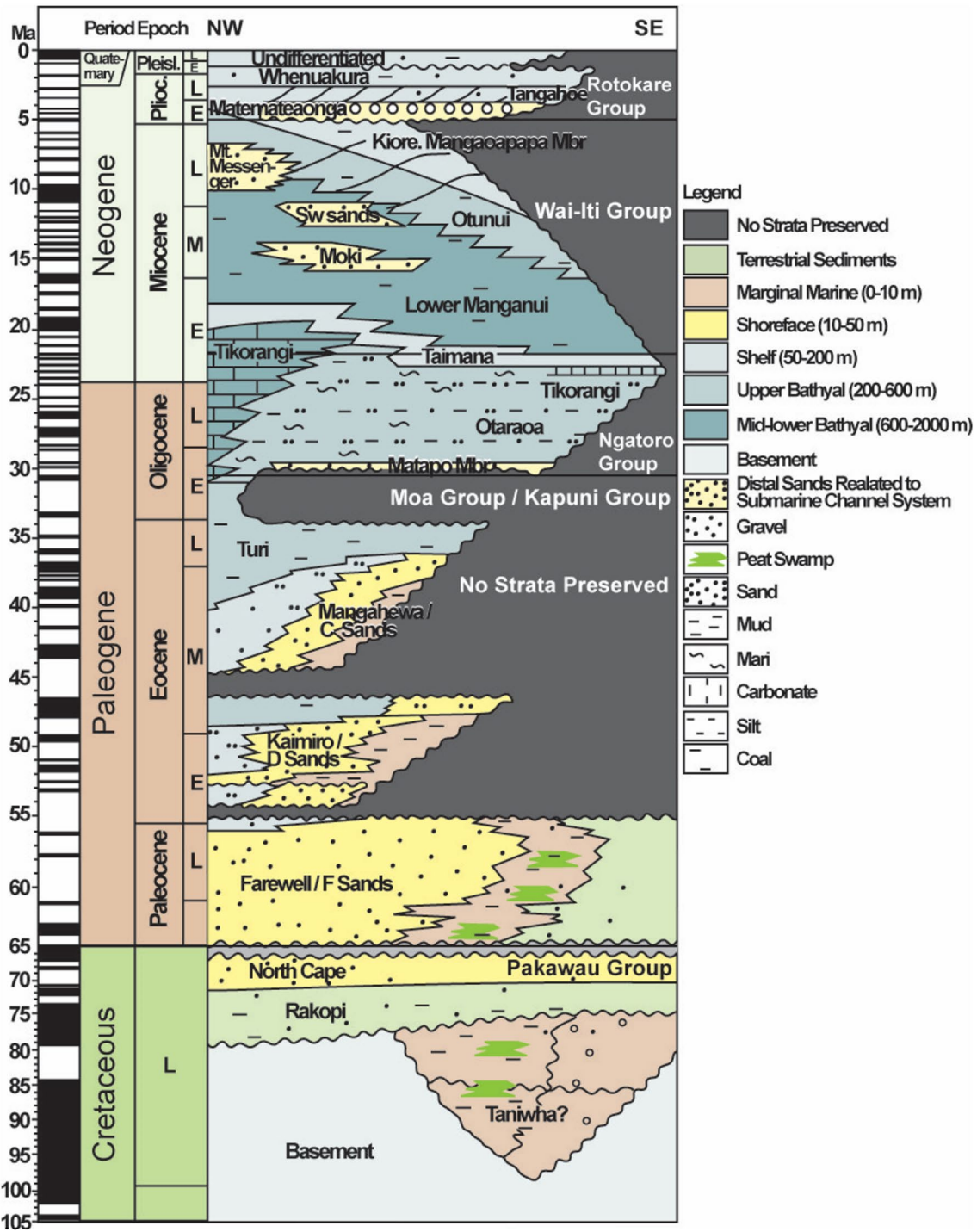


Fig. 2 A stratigraphic succession illustrating a complex and variable cycle of deposition throughout the study area (modified after King and Thrasher 1996)

and vice versa. Eq. (4) given below was used to estimate the hydrocarbon saturation within the reservoir.

$$\text{Hydrocarbon saturation} = 1 - S_w \tag{4}$$

Net pay is another critical factor, which influences the reservoir character. To assess the net-pay i.e., differentiate between water-wet and hydrocarbon-bearing zones, a 50% water saturation cutoff was utilized.

Table 1 (continued)

| Well name | Depth (m) | Plug number | Texture | Grain (%) | | | | | | | | | | Cement | | | | Vpor (%) | | | | | | |
|-----------|-----------|-------------|---------|------------|---------------|---------------|-------|--------|----------|-------------|------|----------|-----|-------------|------|----------------|------|----------|------|-----|-----|-----|------|------|
| | | | | Grain size | | Grain sorting | | Quartz | | Chert | | Feldspar | | Plagioclase | | Rock fragments | | | Mica | H-M | Opq | Cbn | Carb | Clay |
| | | | | Grain size | Grain sorting | Quartz | Chert | K | Feldspar | Plagioclase | Irf | Mrf | Srf | Mica | H-M | Opq | Cbn | | | | | | | |
| KS-4 | 3059.44 | 17 | CL | G | 50 | 1.8 | 0.9 | 3.4 | 1.2 | 1.5 | Tr | Tr | 0.6 | Tr | 3.7 | 28 | 2.7 | | | | | | | |
| KS-4 | 3067.70 | 27 | ML | V-G | 28.3 | Tr | 7 | 9.6 | 1.3 | 1.3 | 0.6 | Tr | 1.9 | Tr | 8.6 | 29.6 | 1.3 | | | | | | | |
| KS-4 | 3068.65 | 31 | ML | G | 32.6 | 0.3 | 6.8 | 10.2 | 1.5 | 1.8 | 1.5 | Tr | 1.8 | Tr | 11.4 | 18.2 | 3.7 | | | | | | | |
| KS-4 | 3070.57 | 39 | MU | G | 31.3 | 0.9 | 3.1 | 7.8 | 1.6 | 2.2 | 1.6 | Tr | Tr | 0.3 | 18.5 | 17.2 | 4.4 | | | | | | | |
| KS-4 | 3071.30 | 41 | MU | G | 33.8 | 4.8 | 9.3 | 9 | 0.6 | 2.1 | 0.9 | Tr | 0.9 | 0.3 | 9.3 | 22.5 | 3 | | | | | | | |
| KS-4 | 3073.67 | 49 | MU | G | 31.3 | 0.6 | 4.2 | 9.6 | 2.1 | 2.7 | 0.9 | 0.3 | 0.6 | Tr | 17.9 | 15.2 | 3.6 | | | | | | | |
| KS-4 | 3076.16 | 53 | CU | G | 50.5 | 2.4 | 3.6 | 12.3 | 1.5 | 2.1 | Tr | Tr | Tr | Tr | 2.4 | 9.9 | 13.8 | | | | | | | |
| KS-4 | 3079.11 | 62 | CL | G | 38.8 | Tr | 7.8 | 12.4 | 1.3 | 1.6 | Tr | 0.3 | 0.3 | Tr | 6.5 | 20.8 | 4.9 | | | | | | | |
| KS-4 | 3085.53 | 72 | CU | G | 38 | 1.5 | 9.9 | 21 | 0.3 | 1.5 | Tr | Tr | 0.3 | 2.1 | 3 | 14.4 | 5.4 | | | | | | | |
| KS-4 | 3085.89 | 73 | CU | M | 38.5 | 1.9 | 7.1 | 19.6 | 1.2 | 9 | 0.3 | Tr | 0.3 | 4.7 | 4.3 | 10.2 | 2.5 | | | | | | | |
| KS-4 | 3089.41 | 77 | V-CL | G | 34 | 2.5 | 4.1 | 31.4 | 1.6 | 4.7 | Tr | Tr | Tr | 0.3 | 5.3 | 11 | 4.7 | | | | | | | |
| KS-4 | 3090.46 | 81 | CL | G | 40.4 | Tr | 13.7 | 11.5 | 1.2 | 2.2 | 0.6 | Tr | 0.3 | 0.9 | 3.4 | 18.6 | 4 | | | | | | | |
| KS-4 | 3094.67 | 88 | MU | M | 37.5 | 0.3 | 7.1 | 9.8 | Tr | 6.8 | 4.1 | Tr | 1 | Tr | 4.1 | 23.6 | 1.4 | | | | | | | |
| KS-4 | 3095.14 | 90 | CL | MG | 35.8 | Tr | 7.6 | 19.6 | 0.6 | 0.9 | 2.5 | 0.3 | 0.3 | Tr | 2.5 | 22.8 | 0.3 | | | | | | | |
| KS-4 | 3096.36 | 95 | CL | MG | 40.5 | 0.3 | 8.8 | 12.8 | 0.9 | 2.7 | 3 | Tr | 0.3 | Tr | 0.9 | 22.3 | 2.7 | | | | | | | |
| KS-4 | 3098.13 | 102 | V-CL | MG | 39 | 0.3 | 10.2 | 26.2 | 4.3 | 3 | Tr | Tr | 0.7 | Tr | 2.3 | 10.5 | 1.6 | | | | | | | |
| KS-4 | 3100.36 | 105 | ML | MG | 27.2 | Tr | 11.6 | 8.1 | Tr | 20.3 | 6.9 | Tr | 1.3 | Tr | 0.6 | 17.2 | Tr | | | | | | | |
| KS-4 | 3103.05 | 109 | CL | M | 38.1 | 0.3 | 8.7 | 9.6 | 1.3 | 1.3 | 2.2 | 0.3 | 1 | Tr | Tr | 23.4 | 3.2 | | | | | | | |
| KS-4 | 3107.06 | 117 | CL | MG | 31.9 | 0.3 | 11.1 | 14.8 | 1.2 | 1.8 | 1.8 | 0.3 | 1.5 | Tr | 0.9 | 17.8 | 4.8 | | | | | | | |
| KS-4 | 3110.17 | 128 | ML | G | 34.6 | Tr | 7.1 | 10.5 | 0.6 | 2.5 | 9.6 | Tr | 0.3 | Tr | Tr | 22.8 | 0.6 | | | | | | | |
| KS-4 | 3111.11 | 132 | CL | MG | 32.5 | Tr | 9.3 | 25.1 | 0.9 | 0.9 | 3.1 | Tr | 0.9 | Tr | Tr | 14.6 | 2.5 | | | | | | | |
| KS-4 | 3114.25 | 143 | MU | MG | 29 | Tr | 10.6 | 10 | 0.6 | 0.3 | 13.9 | 0.3 | 0.9 | Tr | Tr | 18.4 | 3.2 | | | | | | | |
| KS-5 | 2893.72 | 1A | CL | MG | 30 | 0.3 | 18 | 5.7 | 3 | 2.7 | 2.7 | 0.3 | 0.3 | Tr | 0.3 | 16.3 | 10 | | | | | | | |
| KS-5 | 2895.30 | 6A | CU | MG | 31 | 0.7 | 15.7 | 7.3 | 2.7 | 1.7 | 1 | 0.3 | Tr | Tr | 0.3 | 11.3 | 11.3 | | | | | | | |
| KS-5 | 2896.70 | 11A | CL | MG | 34.7 | 0.7 | 16.7 | 4.3 | 2 | 2.3 | 1 | Tr | Tr | Tr | 6.3 | 11.3 | 9 | | | | | | | |
| KS-5 | 2897.92 | 15A | CU | MG | 31.7 | Tr | 14 | 10 | 2 | 4.3 | Tr | Tr | Tr | Tr | Tr | 7.7 | 14 | | | | | | | |
| KS-5 | 2899.36 | 19A | MU | G | 30 | 0.7 | 12.7 | 5.7 | 2.3 | 1.3 | 1.3 | 0.3 | 0.7 | Tr | 10 | 5.7 | 5.7 | | | | | | | |
| KS-5 | 2901.38 | 25A | CL | G | 32 | 1 | 11 | 7 | 2 | 2.3 | 3 | Tr | 0.7 | Tr | 1 | 13.3 | 11.7 | | | | | | | |
| KS-5 | 2903.13 | 31A | CL | G | 34.5 | 0.3 | 11 | 4.5 | 1.9 | 1.6 | 1.9 | 0.6 | 1 | Tr | Tr | 8.4 | 15.5 | | | | | | | |
| KS-5 | 2904.42 | 35A | CL | G | 30.3 | 1 | 15.7 | 8.3 | 3.3 | 3.7 | 0.7 | 0.7 | Tr | Tr | Tr | 6.7 | 14.7 | | | | | | | |
| KS-5 | 2906.42 | 39A | FU | G | 19 | Tr | 9 | 3 | 1.7 | 4.3 | 18 | Tr | 2.3 | Tr | 0.7 | 27.7 | 5.3 | | | | | | | |

Table 1 (continued)

| Well name | Depth (m) | Plug number | Texture | | Grain (%) | | | | | | | Cement | | | | Vpor (%) | | |
|-----------|-----------|-------------|------------|---------------|-----------|-------|----------|-------------|----------------|-----|-----|--------|-----|-----|-----|----------|--------|------|
| | | | Grain size | Grain sorting | Quartz | | Feldspar | | Rock fragments | | | Mica | H-M | Opq | Cbn | | Cement | |
| | | | | | Quartz | Chert | K | Plagioclase | Irf | Mrf | Srf | | | | | | Carb | Clay |
| KS-5 | 2907.91 | 44A | ML | G | 24.7 | 0.3 | 12.7 | 14 | 2.3 | 1.7 | 3 | 7 | 1 | 2.3 | Tr | Tr | 26.7 | 4.3 |
| KS-5 | 2909.58 | 49A | CL | M | 26 | 1 | 16.7 | 16 | 4 | 3.3 | 2.3 | 1.3 | 0.7 | Tr | Tr | Tr | 8 | 20.7 |
| KS-5 | 2910.59 | 52A | CU | M | 30.7 | 0.3 | 17.7 | 14.7 | 6.7 | 1.7 | 1 | 0.7 | 0.3 | Tr | Tr | Tr | 3 | 20 |

Grain size is much variable i.e., medium lower (ML), medium upper (MU), coarse lower (CL), coarse upper (CU) and fine upper (FU). Grain sorting also varies showing moderate (M), good (G), moderately good (MG) and very good (V-G). Rock fragments are abbreviated as igneous (Irf) metamorphic (Mrf) and sedimentary rock fragments (Srf). Heavy minerals and trace amount contents are abbreviated as H-M and Tr, respectively

Results and discussion

Sedimentological analysis

i. Texture

The Farewell Formation shows a variable texture indicating fine to very coarse-grained sandstone intercalated with shale and carbonate as the subordinate lithology, shown in Fig. 3. The details derived from Table 1 indicate that the 48% of the data sets are medium to coarse-grained, 42% samples reveal fine to medium grain size, 6% indicate very fine to fine-sized grains whereas only 4% appeared as coarse to very coarse grained.

ii. Detrital mineralogy

The detrital mineralogy of the Farewell sandstones is classified based on scheme devised by Pettijohn et al. 1987. According to this scheme, the Farewell Formation displays feldspathic arenite to lithic arenite character. A ternary plot shown in Fig. 4 is designed by quantifying the three major detrital constituents i.e., quartz, feldspar and lithic fragments, when added give a total of 100%. This plot shows that the detrital mineralogy is mainly comprising quartz (18.8% to 54.3%). The concentration of feldspar is observed between 4.4% and 38.8%, while the concentration of the chert in the studied samples ranges from 0.3% to 9.3%. Similarly, the lithic fragments and heavy minerals range between 3.1 and 37.7% and 0.3–2.9%, respectively. The concentration of Mica is also observed between 0.3 and 18%.

iii. Porosity, permeability and total cement

The results derived from Table 2 indicate significant porosity ranges between 10.9 and 26.2%, whereas the permeability lies between 0.43 and 1376 mD. Figure 5a, b shows the relationship between the total number of samples with their corresponding porosity and permeability, respectively. A strong poro-perm relationship is also shown in Fig. 6a indicating the Farewell sandstone can accumulate and transmit the hydrocarbons, thus exhibits the reservoir characteristics. The Levorsen classification scheme (Levorsen 1972) when applied to the porosity and permeability data sets, verified the reservoir character of the Farewell sandstones. Figure 6b demonstrates a negative correlation between porosity and total cement content, indicating the increase in the cement content will reduce the pore spaces, thus hindering the reservoir quality of the Farewell Formation. These statistical analyses illustrate a good range of total and effective porosity as well as permeability thus implying toward good reservoir quality of the Farewell Formation.

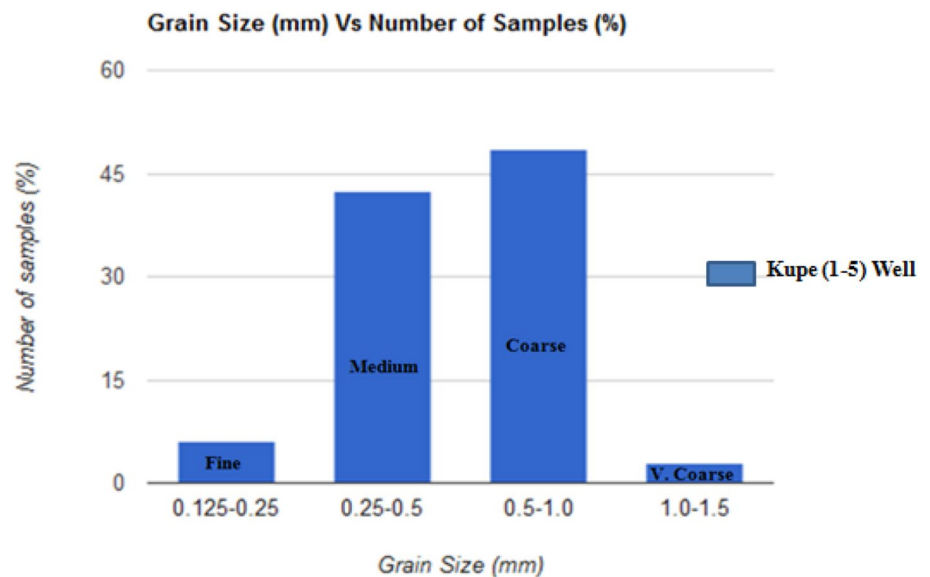
Table 2 The petrographic data sets illustrating the important reservoir parameters derived from the studied wells encountering Farewell Formation within the Kupe Gas Field (provided by MBIE, New Zealand)

| Well name | Depth (m) | Porosity (%) | Permeability (mD) | Total cement (%) | Grain size (mm) |
|-----------|-----------|--------------|-------------------|------------------|-----------------|
| KS-1 | 3141.50 | 20.4 | 20.00 | 18.2 | 0.33 |
| KS-1 | 3147.85 | 19.8 | 4.20 | 15.4 | 0.30 |
| KS-2 | 3083.60 | 17.8 | 11.00 | 25.4 | 0.44 |
| KS-2 | 3086.21 | 16.4 | 19.00 | 20.3 | 0.56 |
| KS-2 | 3091.00 | 15.6 | 16.00 | 17 | 0.66 |
| KS-2 | 3092.80 | 24.8 | 18.00 | 18.1 | 0.76 |
| KS-2 | 3103.30 | 13.8 | 3.20 | 27.9 | 0.40 |
| KS-2 | 3108.70 | 14.5 | 4.30 | 24 | 0.54 |
| KS-2 | 3111.25 | 13.0 | 1.80 | 29.6 | 0.25 |
| KS-2 | 3115.20 | 11.9 | 1.60 | 20.2 | 0.70 |
| KS-2 | 3120.23 | 13.7 | 0.43 | 30.7 | 0.18 |
| KS-2 | 3125.00 | 17.6 | 5.30 | 35 | 0.37 |
| KS-2 | 3127.40 | 21.9 | 82.00 | 12.2 | 0.46 |
| KS-2 | 3128.30 | 17.5 | 13.00 | 14.6 | 0.43 |
| KS-2 | 3150.50 | 22.4 | 87.00 | 16 | 0.39 |
| KS-2 | 3154.40 | 20.5 | 7.90 | 19.6 | 0.25 |
| KS-2 | 3156.20 | 21.1 | 62.00 | 15.6 | 0.44 |
| KS-2 | 3156.79 | 19.2 | 212.00 | 9.9 | 0.63 |
| KS-2 | 3157.40 | 22.3 | 419.00 | 9.7 | 0.55 |
| KS-2 | 3174.84 | 16.9 | 1.20 | 32.9 | 0.18 |
| KS-2 | 3176.00 | 21.6 | 5.10 | 29.7 | 0.23 |
| KS-2 | 3177.21 | 18.5 | 14.00 | 11.4 | 0.39 |
| KS-3B | 3308.00 | 24.3 | 26.00 | 24.6 | 0.36 |
| KS-3B | 3313.00 | 26.2 | 36.00 | 30 | 0.39 |
| KS-3B | 3332.00 | 23.4 | 74.00 | 29.3 | 0.50 |
| KS-3B | 3335.00 | 22.4 | 48.00 | 24 | 0.63 |
| KS-3B | 3377.00 | 22.3 | 18.00 | 22.3 | 0.64 |
| KS-4 | 3052.78 | 17.8 | 28.00 | 27.8 | 0.48 |
| KS-4 | 3054.05 | 22.5 | 327.00 | 16.5 | 0.64 |
| KS-4 | 3056.04 | 19.2 | 17.00 | 27.8 | 0.39 |
| KS-4 | 3057.83 | 19.5 | 36.00 | 21.2 | 0.42 |
| KS-4 | 3058.05 | 15.6 | 21.00 | 20.2 | 0.56 |
| KS-4 | 3059.44 | 13.3 | 2.40 | 31.7 | 0.52 |
| KS-4 | 3067.70 | 17.0 | 5.30 | 38.2 | 0.31 |
| KS-4 | 3068.65 | 14.4 | 2.60 | 29.6 | 0.30 |
| KS-4 | 3070.57 | 13.7 | 4.10 | 35.7 | 0.43 |
| KS-4 | 3071.30 | 16.0 | 7.30 | 31.8 | 0.39 |
| KS-4 | 3073.67 | 12.2 | 1.90 | 33.1 | 0.47 |
| KS-4 | 3076.16 | 18.2 | 130.00 | 12.3 | 0.80 |
| KS-4 | 3079.11 | 15.8 | 4.40 | 27.3 | 0.50 |
| KS-4 | 3085.53 | 16.6 | 17.00 | 17.4 | 0.86 |
| KS-4 | 3085.89 | 13.4 | 4.50 | 14.6 | 0.86 |
| KS-4 | 3089.41 | 13.5 | 9.90 | 16.3 | 1.00 |
| KS-4 | 3090.46 | 15.3 | 4.70 | 22 | 0.62 |
| KS-4 | 3094.67 | 10.9 | 0.76 | 27.7 | 0.44 |
| KS-4 | 3095.14 | 13.8 | 1.80 | 25.3 | 0.58 |
| KS-4 | 3096.36 | 14.0 | 1.30 | 23.3 | 0.58 |
| KS-4 | 3098.13 | 13.9 | 3.10 | 12.8 | 1.25 |
| KS-4 | 3100.36 | 13.8 | 2.50 | 17.8 | 0.30 |
| KS-4 | 3103.05 | 16.8 | 11.00 | 23.4 | 0.52 |

Table 2 (continued)

| Well name | Depth (m) | Porosity (%) | Permeability (mD) | Total cement (%) | Grain size (mm) |
|-----------|-----------|--------------|-------------------|------------------|-----------------|
| KS-4 | 3107.06 | 14.7 | 3.40 | 18.7 | 0.53 |
| KS-4 | 3110.17 | 13.3 | 1.30 | 22.8 | 0.32 |
| KS-4 | 3111.11 | 15.2 | 8.20 | 14.6 | 0.65 |
| KS-4 | 3114.25 | 14.5 | 3.20 | 18.4 | 0.36 |
| KS-5 | 2893.72 | 22.9 | 31.00 | 16.6 | 0.50 |
| KS-5 | 2895.30 | 21.4 | 115.00 | 11.6 | 0.75 |
| KS-5 | 2896.70 | 18.4 | 14.00 | 17.6 | 0.55 |
| KS-5 | 2897.92 | 21.7 | 187.00 | 7.7 | 0.80 |
| KS-5 | 2899.36 | 19.0 | 24.00 | 20 | 0.40 |
| KS-5 | 2901.38 | 21.5 | 62.00 | 14.3 | 0.50 |
| KS-5 | 2903.13 | 21.6 | 303.00 | 8.4 | 0.60 |
| KS-5 | 2904.42 | 22.1 | 278.00 | 6.7 | 0.70 |
| KS-5 | 2906.42 | 20.5 | 14.00 | 28.4 | 0.18 |
| KS-5 | 2907.91 | 21.6 | 6.80 | 26.7 | 0.27 |
| KS-5 | 2909.58 | 24.2 | 651.00 | 8 | 0.50 |
| KS-5 | 2910.59 | 23.5 | 1376.00 | 3 | 0.75 |

Fig. 3 Histogram displaying the relationship between the number of analyzed samples and the size of the grains

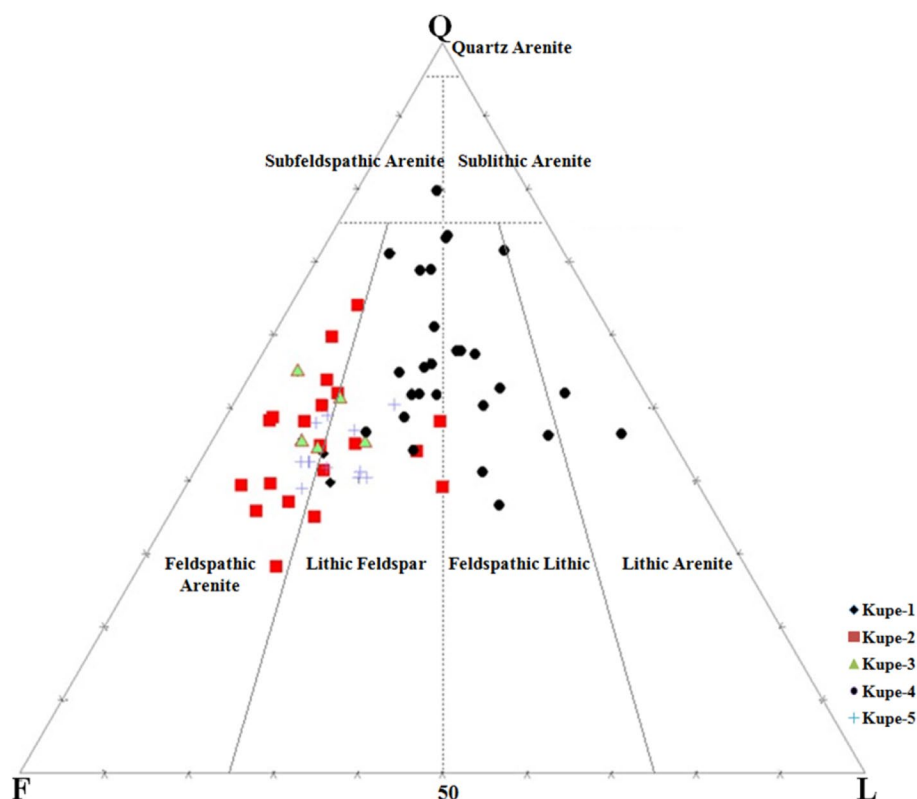


Diagenetic cement and reservoir quality

The data sets shown in Table 1 show that the Farewell Formation is not a clean sandstone rather contains carbonate and authigenic clay contents. The presence of the carbonate is lower (up to 18%) than the clay cement which is 35% of the total cement content as shown in Table 1. The thorium (Th) versus potassium (K) cross-plot is used to identify the different types of clay minerals following the work by Tiyan and Ayers (2010). These clay minerals obstruct the pore spaces and impede the reservoir quality. A strong inverse

relationship is observed between clay cement and porosity, as shown in Fig. 7. Moreover, Fig. 8 shows the presence of a variety of clay minerals i.e., kaolinite, chlorite, illite, mica (biotite), glauconite and montmorillonite. The data points clustered mostly around the chlorite, kaolinite and montmorillonite zones while few points clustered around mica, illite and glauconite. The kaolinite has a crystalline structure, with the book-like appearance and occurs as vermiform particles inside the pores and reduce the reservoir quality. Similarly, the chlorite develops as a radial overgrowth and prevents the further diagenesis of the detrital grain (Worden and Burley 2003). Montmorillonite appears in the form of small crystals and fills the pore lining, thus impeding the

Fig. 4 The QFL diagram based on the classification scheme devised by Pettijohn et al. 1987, showing the distribution of the major detrital components within the Farewell sandstone



reservoir quality (Worden and Burley 2003). The presence of kaolinite, mica and chlorite is also verified from the photomicrographs shown in Fig. 9 and 10. Although the clay minerals deposition within the pore spaces is hostile to the reservoir characteristics, there is a positive aspect related to their deposition (Taylor et al. 2004). For instance, the presence of chlorite prevents the quartz cementation whereas the occurrence of kaolinite can imply to the high porosity zones within the reservoir formation. Kaolinite resulting from acid dissolution during the diagenetic phases also creates secondary porosity (Jiang 2012; Qadri et al. 2019b). In addition to the burial diagenetic processes which impede the reservoir quality, few diagenetic phenomena enhance the porosity and permeability using fracturing, cement dissolution, etc. The presence of secondary and hybrid pores resulting from the feldspar dissolution are verified by Figs. 9 and 10. The present study indicates that although diagenetic types of cement have obstructed the pore spaces, yet the occurrence of secondary and hybrid pores not only minimized the impact of the clay authogenesis but also improved the reservoir character.

Well log analysis

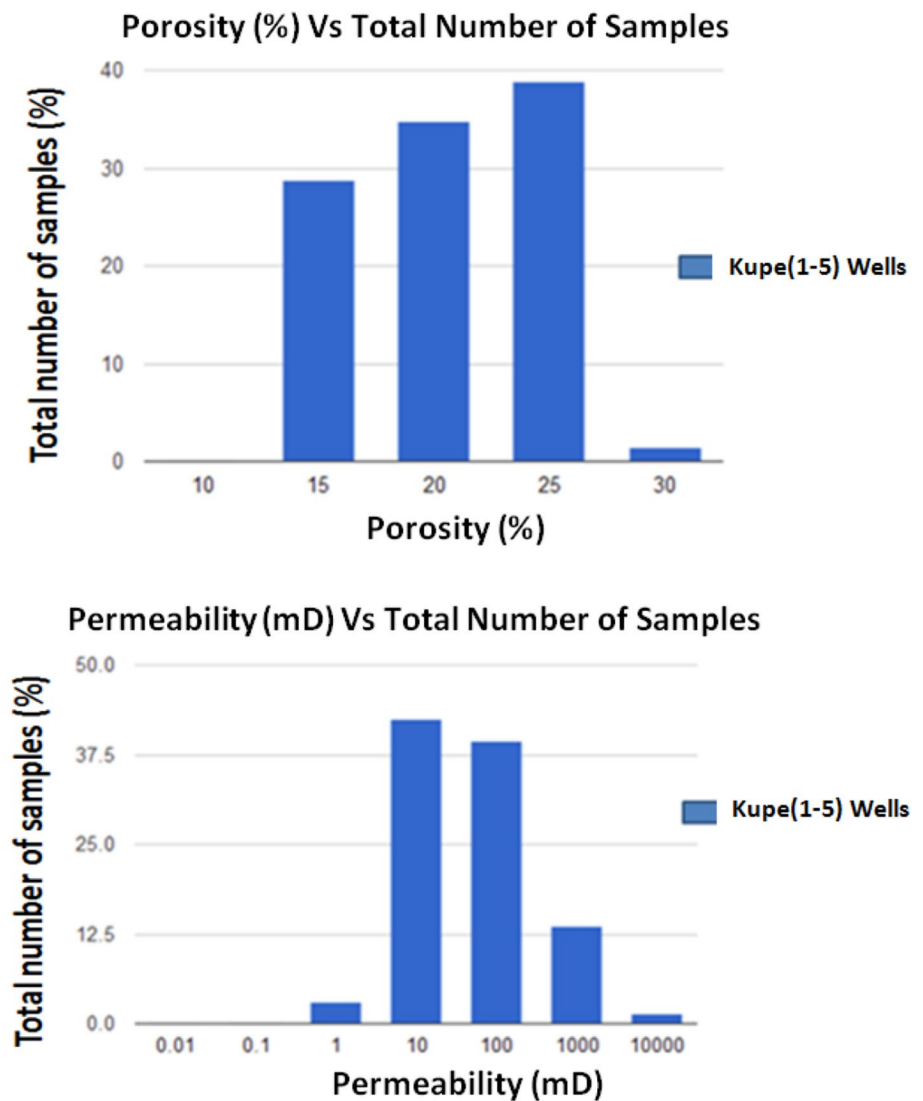
To cross-check the reservoir quality of the Farewell Formation, well log petrophysical analysis was also performed on Kupe South-1, 2, 5 and 7 wells. The Interactive Petrophysics

2013 software was extensively used to execute qualitative and quantitative petrophysical analyses. The qualitative analysis was conducted to identify the lithological and mineralogical composition of the reservoir formation, by plotting the neutron against density logs (Fig. 11), gamma-ray against the neutron logs (Fig. 12) and the M–N cross-plots shown in Fig. 13. The relationship between neutron and density logs revealed the clean to shaly sand nature of the reservoir formation while the shale and carbonate contents act as the subordinate lithological components.

The gamma-ray and neutron log relationship verify the above-mentioned finding and display four data cluster, as shown in Fig. 12. The data constellation displaying lower gamma-ray (less than 45 API) and intermediate values of neutron log points toward clear sandstone, whereas the medium range of gamma-ray and neutron log values indicate the shaly sandstone character. Similarly, the data sets illustrating intermediate gamma-ray log value and higher values from neutron logs (up to 25) show carbonate domination, whereas the data sets with higher gamma-ray (greater than 65 API) and elevated levels of neutron log (above 25) reveal the shale rich contents.

The results from the M–N cross-plot shown in Fig. 13 were consistent with the findings from neutron versus density (Fig. 11) and gamma-ray versus neutron log (Fig. 12) cross-plots, indicating sandstone to shaly sandstone nature

Fig. 5 The histogram displays the link between **a** porosity (%) and **b** permeability mD with the number of analyzed samples in the study



of the reservoir formation with the intercalations of carbonate and shale.

The quantitative petrophysical analysis helped estimate the influential reservoir parameters i.e., the thickness of sand intervals, shale concentration, total and effective porosity, water wetness and hydrocarbon accumulations. Table 3 highlights the findings from the quantitative interpretation. Neutron log-derived porosity and density log-derived porosity were plotted to understand the nature of shale distribution throughout the reservoir formation. The results shown in Fig. 14 revealed the domination of dispersed shale, whereas some of the data constellations also indicated laminated and structural nature of the shale. The occurrence of dispersed shale can be a reason for inaccurate calculations of water and hydrocarbon saturation, that is why we applied the dual water saturation model to the studied wells to achieve accuracy in hydrocarbon calculations.

To calculate a precise shale volume, it is important to separate the shale-rich zones from the sand-rich intervals. Therefore, a 50% shale content cutoff was used, which indicated the V_{sh} ranging between 10.9 and 29% in the analyzed wells. Figure 15 indicates the total porosity established by the neutron-density porosity versus sonic porosity chart, generally, the data clusters showed the intergranular and secondary porosity. The results were consistent with the findings inferred from the petrographical and diagenetic analyses. After applying 10% porosity cutoff, the total porosity observed for the studied wells ranged between 19 and 32.3%, whereas the effective porosity calculations from the studied wells ranged between 17 and 27%.

Similarly, the application of 50% water saturation cutoff helped in discriminating the hydrocarbon-bearing zones from water saturation zones. The Farewell Formation showed a water saturation values between 22.3 and 44.9

Fig. 6 A graphical illustration of the statistical relation between porosity and **a** permeability (mD) and **b** total cement contents (%)

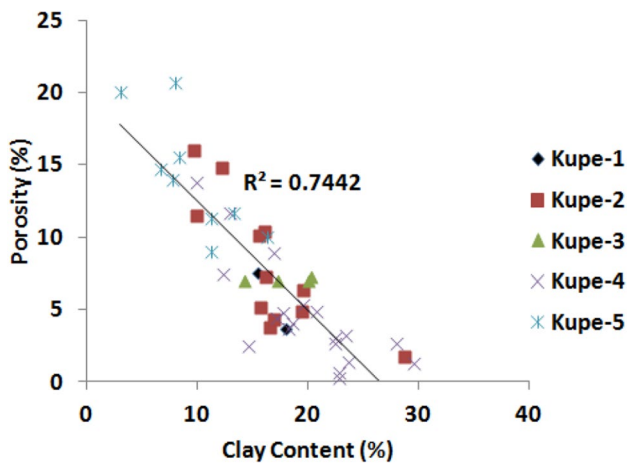
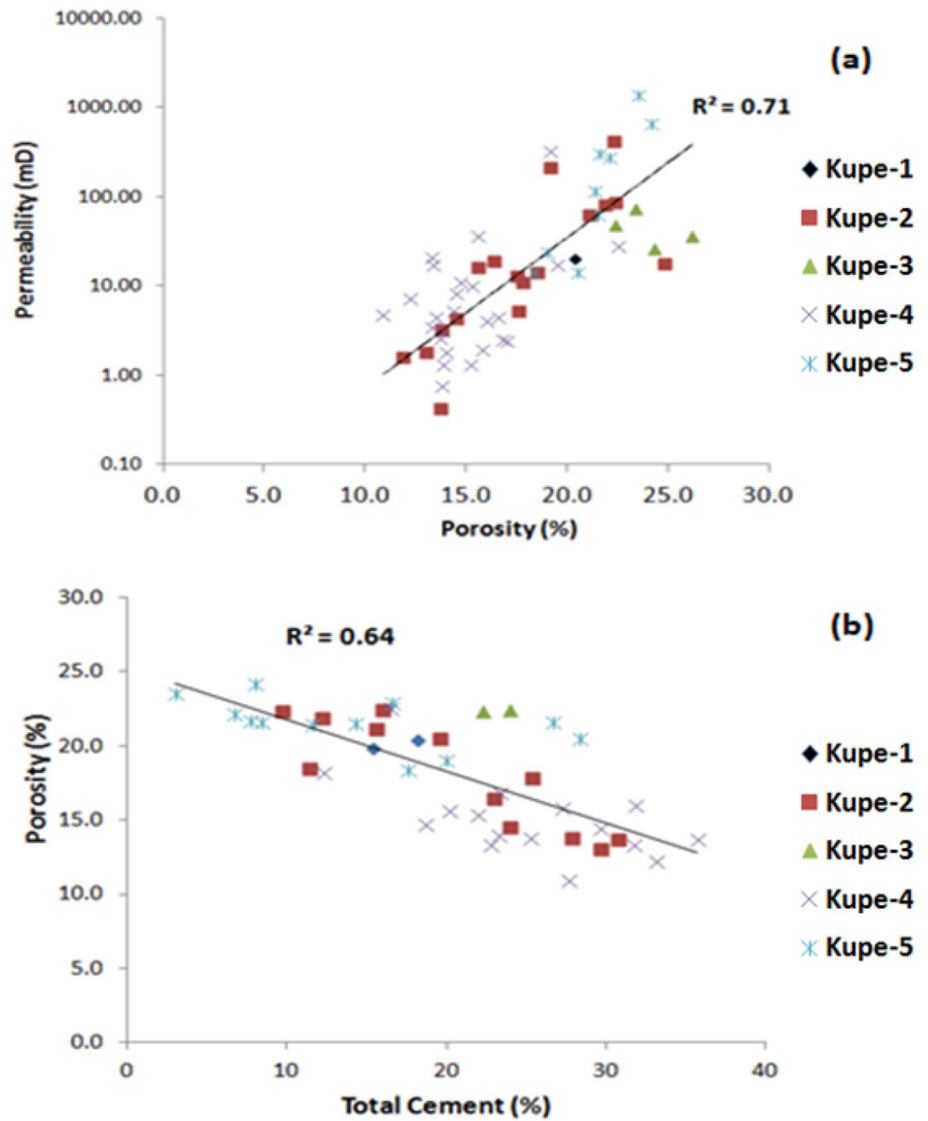


Fig. 7 A graphical demonstration of the strong inverse relationship between clay contents (%) and the porosity (%)

from the studied wells and were later applied to Eq. (4) to calculate the hydrocarbon accumulation. The results highlighted the presence of hydrocarbon fluctuating from 55.1 to 77.7% in the analyzed wells. Table 3 indicates the gross thickness of the Farewell Formation package fluctuating between 165.1 and 480 m whereas the aggregate thickness of the net reservoir zones between 35.7 and 130.5 m. Nine pay zones were identified within the four analyzed wells indicating significant hydrocarbon accumulation, which were combined to calculate the thickness of the total net pay zone for each well, fluctuating from 11.1 to 108.6 m. Figure 16 showed the presence of the sand zones variation in the petrophysical parameters and their distribution throughout the formation whereas Fig. 17 showed the sand zones (green) and net pay zones (red) within the reservoir formation encountered in Kupe South-7 well. The work done by Worthington (2010) illustrates the three

Fig. 8 The identification of variable clay minerals deposited during diagenetic phases are illustrated by plotting thorium log (ppm) values against the potassium log (%) values

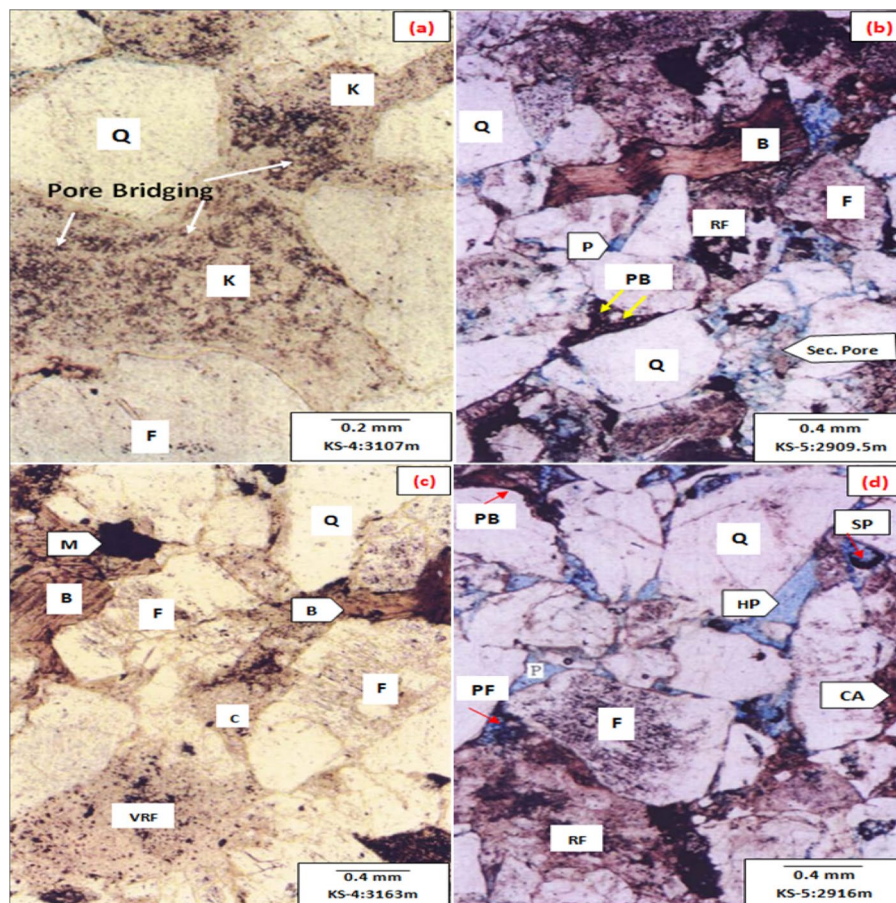
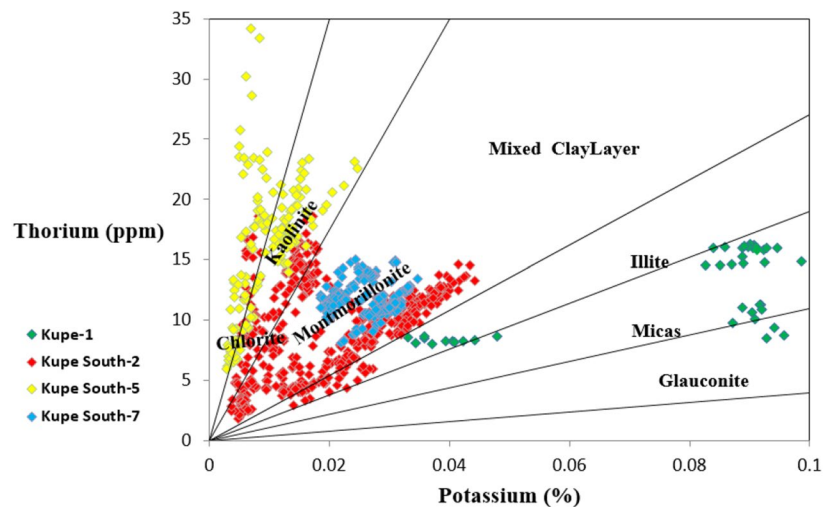


Fig. 9 The photomicrograph derived from the reservoir formation data indicates **a** the image shows Quartz and Feldspar as the main detrital components. Kaolinite (K) is obstructing the pore spaces and thus reducing the porosity and hindering the reservoir quality. **b** The photomicrograph displays good reservoir quality due to the intergranular porosity (P) and secondary pores resulting from feldspar dissolution. Quartz (Q), feldspar (F) and rock fragments (RF) can be seen in the image. Pore bridging (PB) phenomena are also observed due to biotite (B) but have not that much affected the reservoir quality.

c The image illustrates a poor reservoir quality due to clay minerals like chlorite (C), biotite and muscovite completely occluding the pores. Quartz (Q) feldspar (F) and volcanic rock fragments (VRF) are also observed as the detrital minerals in the photomicrograph. **d** The image displays a very good reservoir quality due to presence of hybrid pores (HP), secondary (SP) and intergranular pores (P). The pore bridging and pore-filling due to rock fragments carbonates and clay can also be seen in the photomicrograph but has not impeded the reservoir quality

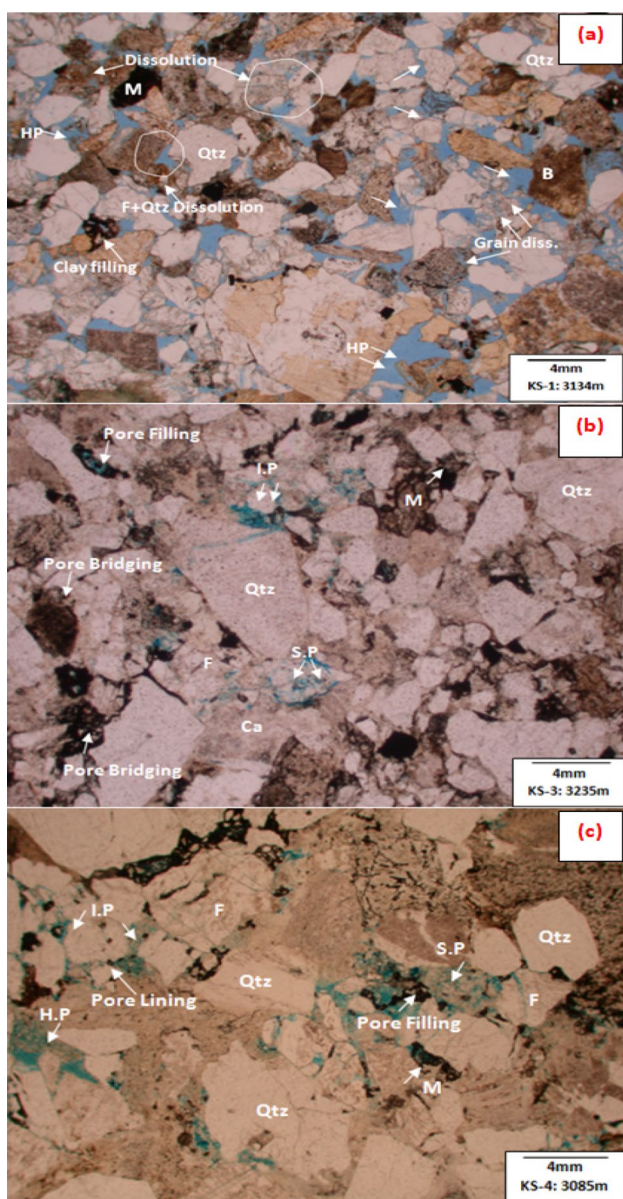


Fig. 10 **a** The poorly sorted, coarse-grain, quartz-bearing sandstone are shown. The connectivity of the intergranular pores is shown. The photomicrograph also indicates the grain dissolution, resulting in secondary and hybrid pores of variable size. The clay filling the pore spaces can also be seen. Overall, the photomicrograph displays a moderate to a good reservoir quality. **b** The photomicrograph indicates the occurrence of quartz and feldspar as the major detrital minerals. The image overall illustrates a poor reservoir quality because of clay and carbonate cement, filling and bridging the pore spaces. The presence of some of the isolated pores can also be seen in the photomicrograph. **c** The photomicrograph illustrates quartz and feldspar as the major detrital components. The presence of intergranular and secondary pore network can also be observed. The photomicrograph demonstrates a fair reservoir quality even though clay minerals are filling the pore spaces

sub-sections of the net to the gross percentage, namely net to the gross sand interval, net to gross reservoir interval and net to gross pay zone. The results derived from the petrophysical analyses showed the variable percentage of the net to gross sand fluctuating from 49 to 72% for the analyzed wells. Similarly, the net to gross reservoir interval was estimated between 34.7 and 57.8%, whereas net to gross pay zone was ranging between 17.8 and 85.9%.

The reservoir quality of the Farewell Formation is evaluated within the Kupe Gas Field by petrophysical study, sedimentological and well log analysis. The investigation established a good relationship between the porosity and permeability thus indicating a good reservoir quality. Based on the sedimentological and petrographical analysis, the texture and detrital mineralogy were established as well as the various diagenetic phases were observed i.e., compaction, cementation, the occurrence of clay minerals in the pore spaces and dissolution. Despite the presence of clay minerals and carbonate cement and their negative impact by impeding the reservoir quality the intense compaction and dissolution processes resulted in the formation of primary and secondary porosities due to which the Farewell Formation exhibited a good reservoir quality. Lastly, the qualitative and quantitative well log analysis revealed that the Farewell Formation showed average effective porosity of 22.2%, moderately low average water saturation of 35% and significant average hydrocarbon saturations of 65% along with good net pay zones. Kupe South-7 well is the most prolific well with the highest thickness of net pay zones (108.6 m) and hydrocarbon saturation (77.7%). The integrated study shows that the Farewell Formation within the Kupe Gas Field exhibits a very good reservoir quality with good reservoir attributes.

Conclusions

- The fine to very coarse-grained, moderately well sorted, Farewell sandstones demonstrate feldspathic arenite to lithic arenite character.
- Well log analysis indicated a very good poro-perm relation indicating the porosity ranging from 10.9 to 26.2% and permeability ranges from 0.43 to 1376 mD, showing the reservoir can accumulate and capability to transmit the hydrocarbon.
- Carbonate and authigenic clay are the major diagenetic cement which has obstructed the pore spaces ranging between 0.2 and 18% and 3–35%, respectively. The impact of these diagenetic cements was minimized due to

Fig. 11 Lithological interpretation of the Farewell Formation from the analyzed wells by plotting neutron log versus density log

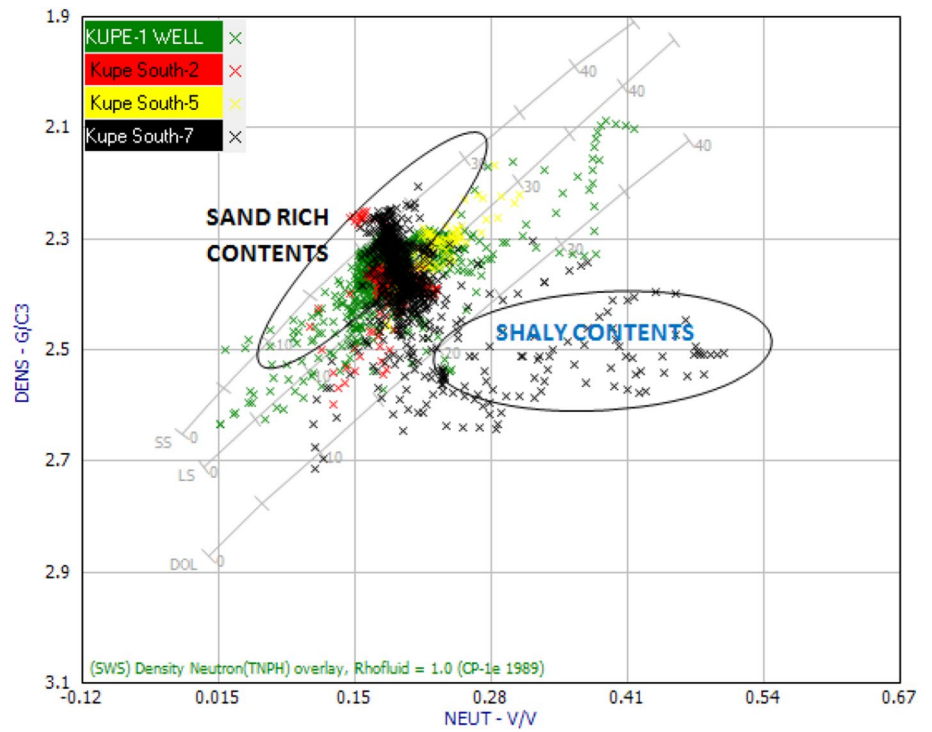


Fig. 12 Neutron log plotted against the gamma-ray log to understand the lithological variations in the reservoir formation

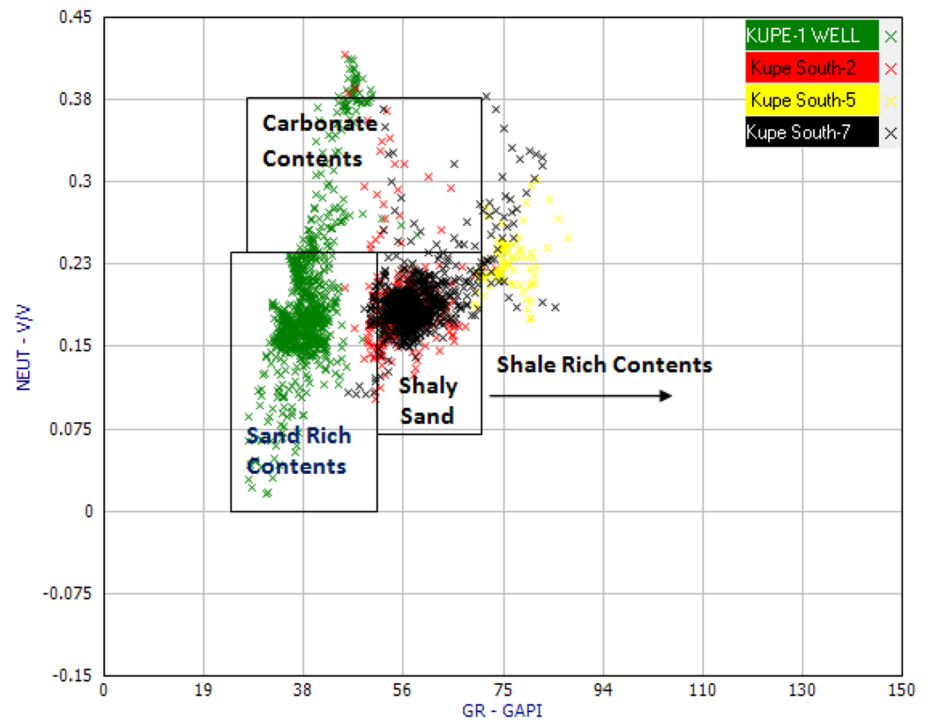


Fig. 13 The illustration of the variable composition of the reservoir formation in the analyzed wells utilizing M–N chart

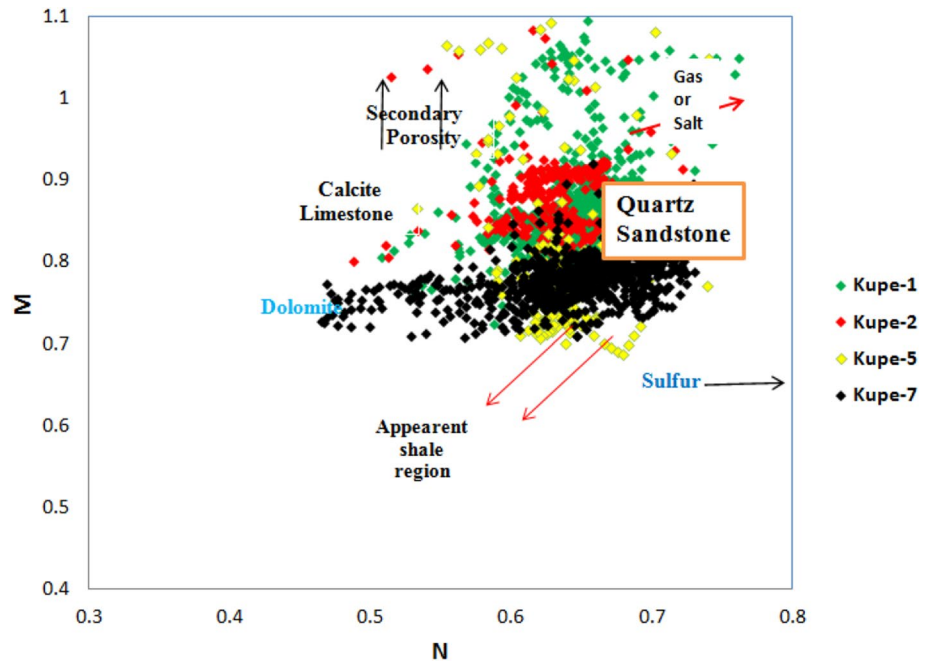


Table 3 The findings from the quantitative well log analysis of the studied wells encountering the Farewell Formation at various depths

| Studied wells | Depth (m) | Total thickness (m) | Reservoir interval (m) | Eff. thickness (m) | Total porosity (%) | Eff. porosity (%) | Shale content (%) | Water wetness (%) | Hydrocarbon saturation (%) |
|---------------|---------------|---------------------|------------------------|--------------------|--------------------|-------------------|-------------------|-------------------|----------------------------|
| Kupe S-1 | 3200- 3680 | 480 | 110 | 22.5 | 31.9 | 27 | 29 | 38.5 | 61.5 |
| Kupe S-2 | 3085.1–3250.2 | 165.1 | 35.7 | 11.1 | 22.1 | 18 | 25.3 | 44.9 | 55.1 |
| Kupe S-5 | 2890.3–3200.5 | 310.2 | 75.2 | 16.2 | 32.3 | 26.2 | 28.1 | 34.3 | 65.6 |
| Kupe S-7 | 3190.5–3500 | 309.5 | 130.5 | 108.6 | 19 | 17 | 10.9 | 22.3 | 77.7 |

V_{sh} indicates the shaly contents, S_w is the water wetness, whereas S_H is the hydrocarbon saturation within the pore spaces

Fig. 14 Neutron-derived porosity plotted against the density-derived porosity to understand the nature of shale dissemination in the studied wells

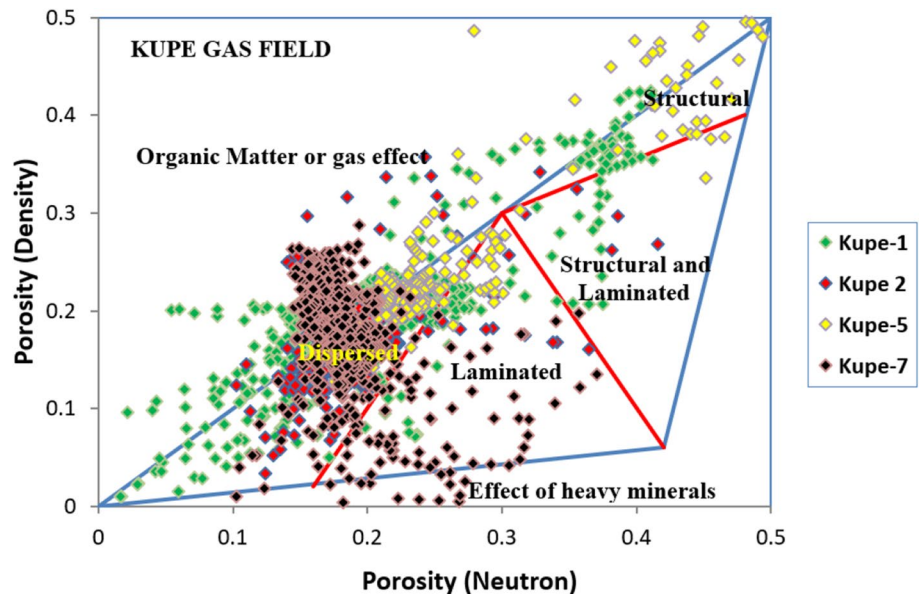
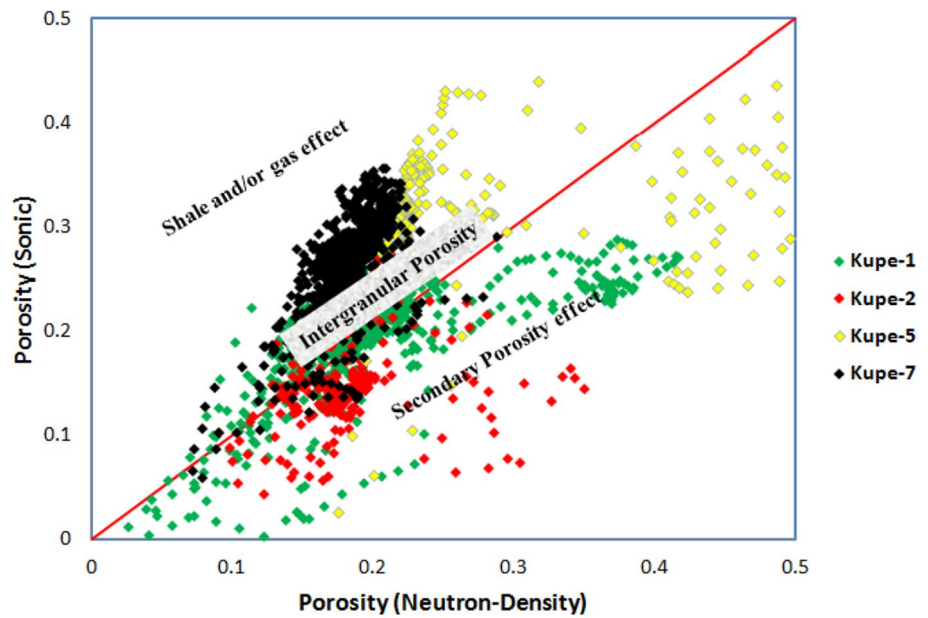


Fig. 15 The neutron-density (porosity) plotted against sonic (porosity) cross-plot indicating the intergranular and secondary porosity as the major types of porosity observed within the analyzed wells



the occurrence of an intergranular, secondary and hybrid type of porosity, thus not impeding the reservoir quality.

- Well log-based petrophysical analysis verified the petrographical analysis indicating sandstone as the major lithological component with shale and carbonates as the subordinate lithology.
- The well log analysis also agreed to the presence of the significant total and effective porosity fluctuating from 19 to 32.3% and 17–27%. These analyses also confirmed the existence of intergranular and secondary porosity.
- The quantitative well log analysis highlighted low shale volume of up to 29%. Water saturation between 44.9 and

22.3% and a substantial hydrocarbon up to 77.7% within the analyzed wells.

- The detailed analysis also verified the nine net pay zones with substantial hydrocarbon accumulation.
- The net to the gross percentage from the pay zones fluctuating between 17.8 and 85.9% also indicates the good reservoir quality.

The findings from the sedimentological and well log-based petrophysical analyses were in good agreement to verify the good reservoir quality of the Farewell Formation.

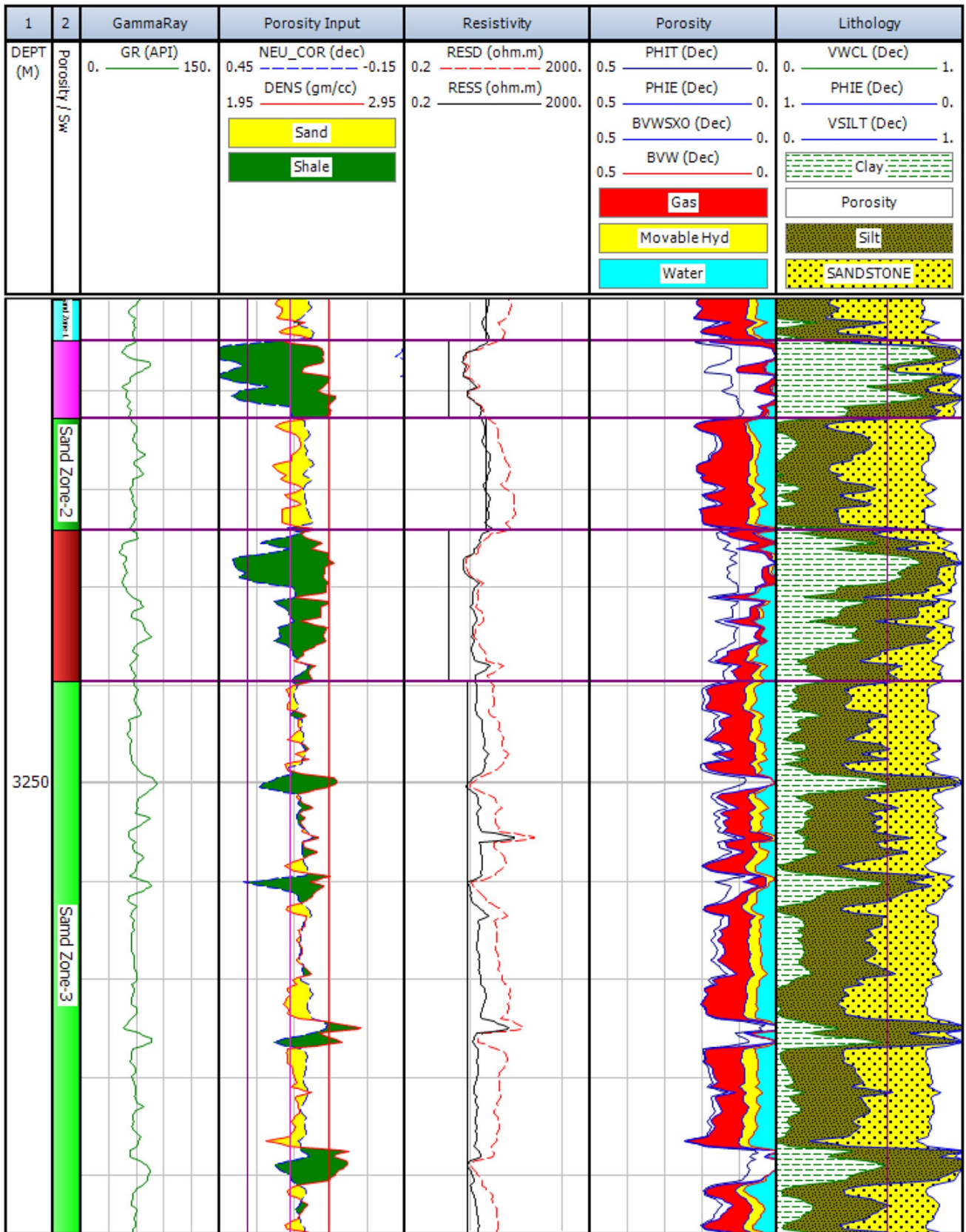


Fig. 16 The vertical distribution of the petrophysical parameters is displayed within the Farewell Formation encountered in the Kupe South-7 well

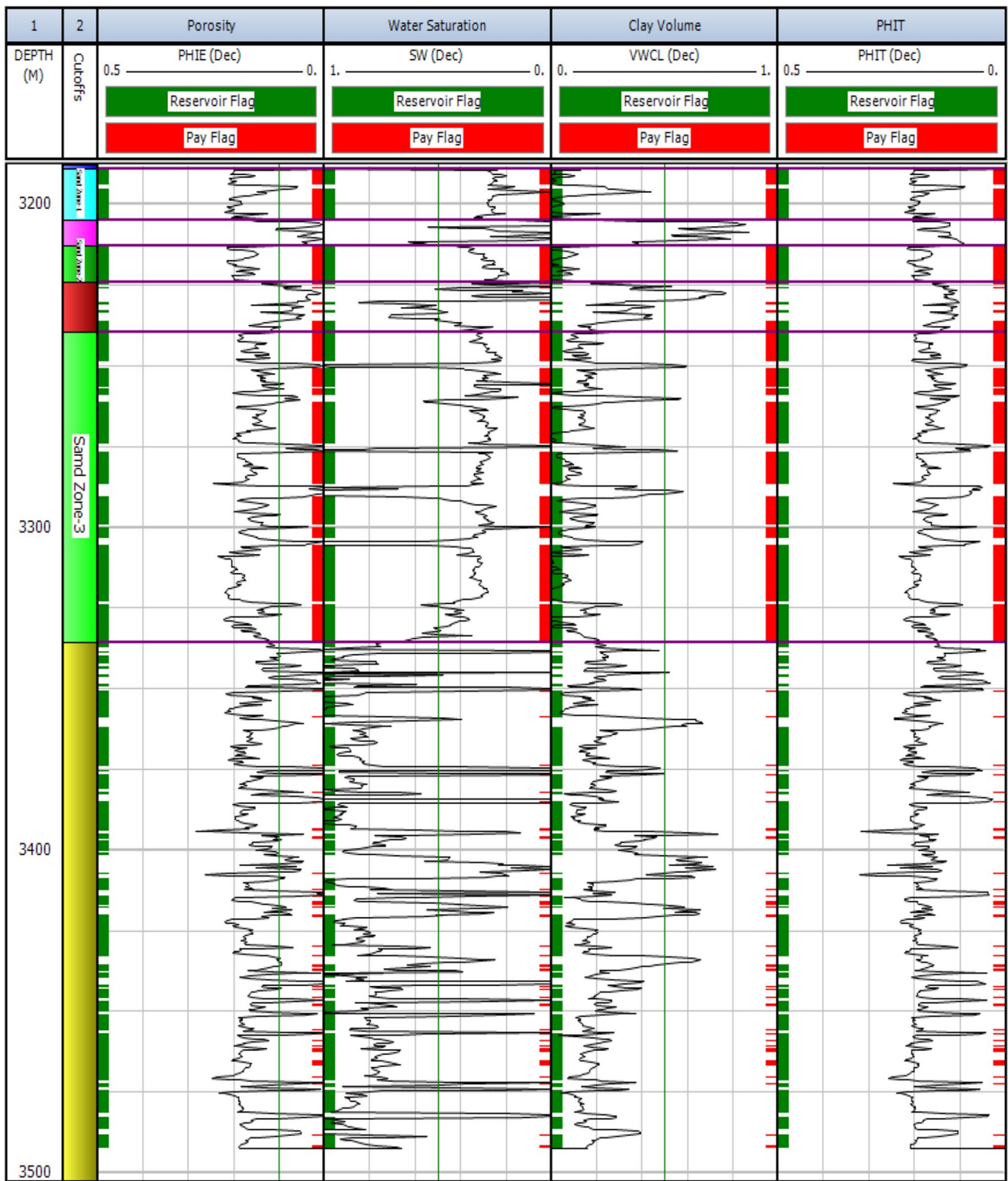


Fig. 17 The reservoir and pay zones are discriminated by the variable colors i.e., green and red shades, respectively. The thickness of the pay zones is quite significant within the sand zones of the Kupe South-7 well

Funding There are no fundings for the study presented in the manuscript.

Compliance with ethical standards

Conflict of interest Authors have no conflict of interest.

Open Access This article is licensed under a Creative Commons Attribution 4.0 International License, which permits use, sharing, adaptation, distribution and reproduction in any medium or format, as long as you give appropriate credit to the original author(s) and the source, provide a link to the Creative Commons licence, and indicate if changes were made. The images or other third party material in this article are included in the article's Creative Commons licence, unless indicated otherwise in a credit line to the material. If material is not included in the article's Creative Commons licence and your intended use is not permitted by statutory regulation or exceeds the permitted use, you will need to obtain permission directly from the copyright holder. To view a copy of this licence, visit <http://creativecommons.org/licenses/by/4.0/>.

References

- Adelua AO, Aderemib AA, Akanij AO, Sanuaded OA, Kakad SI, Afolabia A, Olugbemigab S, Okeb R (2019) Application of 3D static modeling for optimal reservoir characterization. *J Afr Earth Sci* 152:184–196
- Al-Jawad SNA, Ahmed MA, Saleh AH (2020) Integrated reservoir characterization and quality analysis of the carbonate rock types, case study, southern Iraq. *J Petrol Explor Prod Technol* 10:3157–3177
- Alotaby WD (2015) Fault interpretation and reservoir characterization of the Farewell Formation within Kerry Field, Taranaki Basin, New Zealand. Master's Thesis. 7458. Missouri University of Science and Technology
- Anthony DP, Gilbert CE, Sutherland GF et al (2005) Kupe central field area (CFA) subsurface development plan, PML 38146, Offshore Taranaki Basin, New Zealand, Unpublished Origin Energy Resources report OF0401-PLN-00-A-0008
- Asquith G, Krygowski D (2004) Basic well log analysis, 2nd edn. AAPG methods in exploration series, 16, p 244
- Dong SP, Shalaby MR, Islam MA (2018) Integrated reservoir characterization study of the McKee formation, onshore Taranaki Basin, New Zealand. *Geosciences* 8:105
- Gier S, Worden RH, Johns WD, Kurzweil H (2008) Diagenesis and reservoir quality of Miocene sandstones in the Vienna Basin. *Austria Mar Pet Geol* 25:681–695
- Griffin AG, Bland KJ, Field B, Strogon DP et al (2015) Reservoir characterization of the east coast and Pegasus Basin, Eastern North Island, New Zealand. In: International conference and exhibition, Melbourne, Australia. 13–16 September 2015, p 150. doi: 10.1190/ice2015-2207834
- Higgs KE, Crouch EM, Raine JI (2017) An interdisciplinary approach to reservoir characterization: an example from the early to middle Eocene Kaimiro Formation, Taranaki Basin, New Zealand. *Mar Pet Geol* 86:111–139
- Higgs KE, King PR, Raine JI, Sykes R et al (2012) Sequence stratigraphy and controls on reservoir sandstone distribution in an Eocene marginal marine-coastal plain fairway, Taranaki Basin, New Zealand. *Mar Pet Geol* 32:110–137
- Islam MA, Yunsi M, Qadri SMT, Shalaby MR, Haque AKME (2020) Three-dimensional structural and petrophysical modeling for reservoir characterization of the Mangahewa formation, Pohokura Gas-Condensate Field, Taranaki Basin, New Zealand. *Nat Resour Res*. <https://doi.org/10.1007/s11053-020-09744-x>
- Islam MA (2009) Diagenesis and reservoir quality of Bhuvan sandstones (Neogene), Titas Gas Field, Bengal Basin, Bangladesh. *J Asian Earth Sci* 35:89–100
- Jiang S (2012) Clay minerals from the perspective of oil and gas exploration. In: Valašcova M, Martynkova GS (eds) Clay minerals in nature-their characterization, modification and application, pp 21–38. <https://doi.org/10.5772/47790>
- Jumat N, Shalaby MR, Islam MA (2018) Integrated reservoir characterization of the Paleocene Farewell Formation, Taranaki Basin, New Zealand, using petrophysical and petrographical analyses. *J Pet Explor Prod Technol* 8:685–701
- King PR, Thrasher GP (1996) Cretaceous-Cenozoic geology and petroleum systems of the Taranaki Basin, New Zealand. In: Institute of Geological and Nuclear Sciences Monograph, vol 13(2). Institute of Geological and Nuclear Sciences, Lower Hutt
- Knox GJ (1982) Taranaki Basin, structural style and tectonic setting. *N Z J Geol Geophys* 25:125–140
- Levorsen LA (1972) Geology of petroleum, 2nd edn. Freeman W.H. and Company Pub, San Francisco, p 724
- Martin KR, Baker JC, Hamilton PJ, Thrasher GP (1994) Diagenesis and reservoir quality of Paleocene sandstones in Kupe South Field, Taranaki Basin New Zealand. *AAPG Bull* 78(4):624–643
- Nabawy BS, Elgendy NTH, Gazia MT (2019) Mineralogic and diagenetic controls on reservoir quality of Paleozoic sandstones, Gebel-El-Zeit, North Eastern Desert, Egypt. *Nat Resour Res*. <https://doi.org/10.1007/s11053-019-09487-4>
- Osinowo OO, Ayorinde JO, Nwankwo CP, Ekeng OM, Taiwo OB (2018) Reservoir description and characterization of Eni field offshore Niger Delta, southern Nigeria. *J Pet Explor Prod Technol* 8(2):381–397
- Pettijohn FJ, Potter PE, Siever R (1987) Sand and sandstone. Springer, New York
- Qadri SMT, Shalaby MR, Islam MA (2016) Source rock characterization and hydrocarbon generation modelling of the middle to late Eocene Mangahewa Formation in Taranaki Basin, New Zealand. *Arab J Geosci* 9:559
- Qadri SMT, Shalaby MR, Islam MA (2017) Seismic interpretation and structural modelling of Kupe Field, Taranaki Basin. *New Zealand: Arab J Geosci* 10:295
- Qadri SMT, Shalaby MR, Islam MA (2019a) Three dimensional petrophysical modelling and volumetric analysis to model the reservoir potential of the Kupe field, Taranaki Basin New Zealand. *Nat Resour Res* 28:369
- Qadri SMT, Shalaby MR, Islam MA (2019b) Application of well log analysis to estimate the petrophysical parameters and evaluate the reservoir quality of the Lower Goru Formation, Lower Indus Basin, Pakistan. *Geomech Geophys Geoenergy Georesour*. <https://doi.org/10.1007/s40948-019-00112-5>
- Raine JI (1984) Outline of a palynological zonation of Cretaceous to Paleogene terrestrial sediments in west coast region, South Island, New Zealand. *New Zealand Geological Survey Report* 109
- Rider M (1996) The geological interpretation of well logs, 2nd edn. Rider French Consulting Ltd., Aberdeen, Sutherland, p 178
- Schmidt DS, Robinson PH (1990) The structural setting and depositional history for the Kupe South Field, Taranaki Basin. In: 1989 New Zealand oil exploration conference proceedings. Ministry of Commerce, Wellington-New Zealand, pp 151–172
- Shalaby MR, Sapri SHB, Islam MA (2020) Integrated reservoir characterization and fluid flow distribution of the Kaimiro Formation, Taranaki Basin, New Zealand. *J Pet Explor Prod Technol* 10:3157–3177
- Soleimani M, Shokri JB, Rafiei M (2017) Integrated petrophysical modelling for a strongly heterogeneous and fractured reservoir, Sarwak Formation, SW Iran. *Nat Resour Res* 26:75–88

- Taylor TR, Stancliffe R, Macaulay CI, Hathon LA (2004) High temperature quartz cementation and the timing of hydrocarbon accumulation in the Jurassic Norphlet sandstone, offshore Gulf of Mexico, U.S.A. In: Cubit JM, England WA, Larter S (eds) Understanding petroleum reservoirs: towards an integrated reservoir engineering and geochemical approach, Geological Society (London) Special Publication 237, pp 257–278
- Tiyan Y, Ayers WB (2010) Barnett Shale (Mississippian), Fort Worth Basin, Texas: regional variations in gas and oil production and reservoir properties CSUG/SPE 137766. In: Canadian unconventional resources and international petroleum conference Calgary, Alberta, Canada, 19–21 October. <https://doi.org/https://doi.org/10.2118/137766-MS>
- Worden RH, Burley SD (2003) Sandstone diagenesis from sand to stone. In: Burley SD, Worden RH (eds) Clastic diagenesis recent and ancient. International Association of Sedimentologists, vol 4. Blackwells, Oxford, pp 3–44
- Worthington PF (2010) Net pay-what is it? what does it do? how do we quantify? how do we use it? SPE Reserv Eval Eng 13(5):812–822
- Wyllie MRJ (1963) The fundamentals of well log interpretations. Academic Press, New York

Publisher's Note Springer Nature remains neutral with regard to jurisdictional claims in published maps and institutional affiliations.